Effect of Nano-size Magnetic Additions on Low Temperature Flux Pinning of Y-Ba-Cu-O Thin Films

M. A. Sebastian, N. A. Pierce, I. Maartense, G. Kozlowski, T. J. Haugan

***Abstract*—Manufacturing of coated conductors can be tailored for future use operating parameters, such as high temperature and low field, mid temperature and mid field and low temperature and high field. Different methods of flux pinning are being tested world-wide to enhance critical currents (I_{cs}) of high temperature superconductor $YBa_2Cu_3O_{7-x}$ (YBCO) coated conductors for these various operating conditions. Magnetic materials are interesting to consider as flux pinning additions because of their potential for very strong pinning strength. This research describes the study of different magnetic phase additions to YBCO including: M = $BaFe_{12}O_{19}$, $La_{0.67}Ca_{0.33}MnO_3$, $Y_3Fe_5O_{12}$, and $SrRuO_3$. Nano-size additions were incorporated by depositing multilayer (M/YBCO)N films to minimize degradation of T_c, and testing volume % additions of M phase from 0.5 % to 5%. Experimental current density ($J_{cm}(H,T)$) results for mid temperature (30 K–65 K) / mid field (1 T–5 T) and low temperature (< 30 K) / high field (> 5 T) will be presented. Microstructural and superconducting properties will be summarized, including SEM & TEM analysis.**

***Index Terms*—critical current density, magnetic flux pinning, superconducting thin films, yttrium barium copper oxide**

I. Introduction

Various applications of high temperature superconductors require different operating temperature and applied fields. Cables operate at high temperature and low fields, motors and generators operate at mid temperature and mid field, while MRI and NMR operate at low temperatures and high fields. Production of HTS films can be tailored to deliver optimized results for each of these operating regimes. Intrinsic pinning and the types of defects introduced by doping the films, can be manipulated to provide the desired scenario. For example, it is now known that "0D" point artificial pinning centers (APCs) are preferred for low temperature and high field performance, "1D" columnar APCs are preferred for high temperatures above 65 K and fields less than 1 T, "3D" APCs are preferred for low temperatures below 30 K and mid fields above 5 T, and mixed defects are the best combination for mid temperatures of 30–65 K and low fields of 1–2 T [1], [2]. A plethora of these incorporated APCs have been researched, such as $BaHfO_3$, $BaZrO_3$, $BaSnO_3$, $Ba_2Y(Nb,Ta)O_6$, Y_2O_3, and Y_2BaCuO_5 nano-rods and nanoparticles [3]–[8]. These APCs and their resulting defects pin the normal cores of the vortices in type II superconductors. This core pinning is however limited by the coherence length of 25 Å. Employing magnetic APCs allows one to take advantage of magnetic pinning, which pins the magnetic flux of the vortices, and is limited by the magnetic penetration depth of 1500 Å. The columnar volume of magnetic pinning is much larger than that of core pinning, and results in the magnetic pinning strength being 100–1000 times the strength of core pinning. When utilizing magnetic dopants in $YBa_2Cu_3O_{7-\delta}$ (YBCO) films, an external magnetic field applied perpendicular to the film results in domain wall movement and magnetic pinning, which is seen as an S–shaped hysteresis loop as opposed to a square shaped one. In the case of perpendicular anisotropy, the magnetic pinning scales with the saturation magnetization; whereas with in-plane anisotropy, magnetic pinning occurs below the coercive field [9]–[13].

Many research groups have explored additional magnetic pinning strength by doping YBCO films with ferromagnetic, anti-ferromagnetic, and ferrimagnetic additions. H. Wang's research groups have investigated doping YBCO with Fe_2O_3, $BaFe_{12}O_{19}$ (BFO), $YFeO_3$, and $La_{0.67}Sr_{0.33}MnO_3$ (LSMO) in single and multilayer films, and employing the use of CeO_2 buffer layers and magnetic cap layers. Their results showed increased pinning effects due to the magnetic additions [14], [15]. Garcia-Santiago *et al.* produced a BFO/YBCO bilayer with a yttria stabilized (YSZ) buffer layer via pulsed laser deposition (PLD), and found that the BFO caused in increased upward shift of the irreversibility line (IL). The results were explained theoretically by Bulaevkii that the applied magnetic field and the demagnetizing field in the BFO layer result in the magnetic field in the YBCO layer. The magnetic domain walls are pinned when the applied field is less than the coercive field for BFO, ~5 kOe [10], [11]. Other research groups have doped YBCO films with $Y_3Fe_5O_{12}$ (YIG) [16], [17]. Colossal magnetoresistance (CMR) compounds of LSMO and $La_{2/3}Ca_{1/3}MnO_3$ (LCMO) were investigated as bilayers and up to 8 layers with YBCO. Results showed significant pinning contributions [12],

(Style: TAS First page footnote) Manuscript receipt and acceptance dates will be inserted here. This work was supported by AFRL / Aerospece System Directorate and the Air Force Office of Scientific Research (LRIR No. 14RQ08COR and No. 18RQCOR100). *(Corresponding author: Mary Ann Sebastian.)*

M. A. Sebastian is with the University of Dayton Research Institute, Dayton, OH 45469 USA (e-mail: mary_ann.sebastian.1.ctr@us.af.mil)

N. A. Pierce was with Wright State University, Dayton, OH 45435 USA. He is now with Hohman Plating & Manufacturing Inc., Dayton, OH 45404 USA (e-mail: npierce@hohmanplating.com)

I. Maartense was with the University of Dayton Research Institute, Dayton, OH 45469 USA, and is now retired.

G. Kozlowski is with Wright State University, Dayton, OH 45435 USA and with UES, Dayton, OH 45432 USA (e-mail: gregry.kozlowski.usa@gmail.com)

T. J. Haugan is with AFRL/RQQM, WPAFB, OH 45431 USA (e-mail: timothy.haugan@us.af.mil)

Color versions of one or more of the figures in this paper are available online at http://ieeexplore.ieee.org.

Digital Object Identifier will be inserted here upon acceptance.

[14], [18]. R. Al-Mohsin found that doping bulk YBCO with $Zn_{0.95}Mn_{0.05}O$ showed evidence of magnetic pinning [19]. Other interesting work was done by V. Rouco with inserting Co nanorods in a YBCO thin film by milling antidots via Ga focused ion beam (FIB) and filling with cobalt via focused electron beam deposition (FEBID). In this study the superconducting stray fields effect the magnetization of the Co nanorods, allowing for tuning of the system to increase current density [20]. F. Colauto also saw that coating a metallic or magnetic layer on low T_c superconductors such as Nb and MgB_2 could help to avoid flux avalanches from thermal instabilities [21]. Another unique paper studied compared the unique pinning mechanism of TmBCO to YBCO, and suggested substituting Fe^{3+} for Y to harness magnetic pinning contributions[22]. Our own research group also previously explored nano-size magnetic additions in multilayer films consisting of 28 and 38 bilayers, which to our knowledge, was many more layers than previously seen in research. Our previous studies investigated current densities in high and mid temperature regimes [23], but did not present data for low temperature regimes. This paper employs the scaling laws for superconductivity and the strong correlation between J_c (77 K, 3 T//c-direction) to attain low temperature data down to 5 K [24]–[25]. New TEM analysis will also be presented.

II. Experimental Details

A. Thin Film Production

Targets utilized in this research were both produced in-house and purchased from commercial suppliers. The YBCO target Nexans powder was pressed with a Carver die press, followed by a sintering process in a box furnace. $BaFe_{12}O_{19}$ (BFO), $La_{0.67}Ca_{0.33}MnO_3$ (LCMO), $Y_3Fe_5O_{12}$ (YIG), and $SrRuO_3$ (SRO) were commercial targets. Further details can be found in previous work [23].

Thin films were produced using the before mentioned targets and $LaAlO_3$ (LAO) and $SrTiO_3$ (STO) substrates via pulsed laser deposition (PLD) with a KrF excimer laser (λ= 248 nm). The YBCO/BFO composite films consist of 28 bilayers, with resulting volume percent additions varying from 0.6, 1.4, and 2.7 vol. %. The YBCO/LCMO composite films also consist of 28 bilayers, but laser repetition rate of 2 Hz rather than 4 Hz resulted in volume percent additions of 0.8, 1.2, and 2.4 vol. %. YBCO/SRO composited films consist of 38 bilayers, with resulting volume percent additions varying from 1.2, 2.4, and 4.7 vol. %. YBCO/YIG composite films also consist of 38 bilayers with volume percent additions of 3.6, 7.0, and 11.1 vol. %. Details in regards to PLD conditions and annealing can be found in previous work. [23].

B. Thin Film Characterization

Film characterization included film thickness determination which involved etching and measurement with a profilometer. Magnetic current density was attained with a Quantum Design Physical Properties Measurement System (PPMS) with a vibrating sample magnetometer (VSM) probe. VSM data was attained for temperatures of 77 K, 65 K, 50 K, 20 K, and 5 K, with applied field applied // to the c-axis of the films from 0–9 T. Magnetic current density analysis involved utilization of the Bean Critical State Model [23], [26]–[28]. Superconducting transition temperature (T_c) was attained via AC susceptibility measurements, and transport current density (J_{ct}) measured on microbridges with a 1 μV/cm criteria. Microstructure was examined with a FEI Sirion Scanning Electron Microscope (SEM), a Bruker D8 Discover diffractometer. Also a Tescan Lyra FIB/SEM was used to prepare foils for YBCO/SRO and YBCO BFO samples for TEM examination with the TALOS TEM SYSTEM FSE. More details can be found in previous work [23].

III. Results & Discussion

Previously, we reported the effects of magnetic nanoparticle addition on the onset critical temperature ($T_{c\text{-}onset}$) and the self-field current density ($J_{ct\ self\text{-}field}$) [23]. Our results showed that increased vol. % BFO dramatically decreased $T_{c\text{-}onset}$ and $J_{ct\ self\text{-}field}$, and increased $T_{c\ FWHM}$, compared to additions of LCMO, SRO, and YIG. It is believed this may be a result of reaction products and strain development due to a higher degree of lattice mismatch with YBCO. SEM also depicted typical island growth and insulating phase nanoparticle charging. XRD analysis also indicated epitaxial growth of YBCO films identified by *(001)* YBCO and substrate peaks [23]. The rest of this paper will present new TEM results and new current density results that were measured in the low to mid temperature regime.

TEM analysis of the YBCO/SRO multilayer film is in very good agreement with the measured film thickness of 236 nm. Elemental analysis clearly shows the La, Al, and O present in the substrate, along with the Y, Ba, Cu, and O present for the YBCO, along with the Ru, and to a lesser extent the Sr. Interestingly, evidence of Y_2O_3 nanoparticles can be seen in areas where Y and O are present, but Ba and Cu are absent (Fig. 1). TEM analysis of The YBCO/YIG multilayer films has a measured thickness of 275 nm. From TEM elemental analysis, La, Al, and O are present in the substrate, along with Y, Ba, Cu, and O present for the YBCO, and Y, Fe, and O present for the YIG. Y_2O_3 nanoparticles also appear to be present in areas where Y and O are present, but Ba and Cu are absent (Fig. 2).

Magnetic current density was previously attained for 77 K, 65 K, and 40 K, but not for the lower temperatures of 20 K and 5 K. Current density values initially attained pre-etch at 65 K, 3 T were used to normalize current densities attained post-etch. This was to account for decreased area of film available after etching for film thickness determination after the initial current density measurements, but prior to the current density measurements at lower temperatures [24], [25]. From Fig. 3, current densities for 65 K, 50 K, 20 K, and 5 K., with the field ramped from 0–10,000 Oe parallel to the c-direction or perpendicular to the film surface, for each of the dopant systems with varied volume percent are presented.

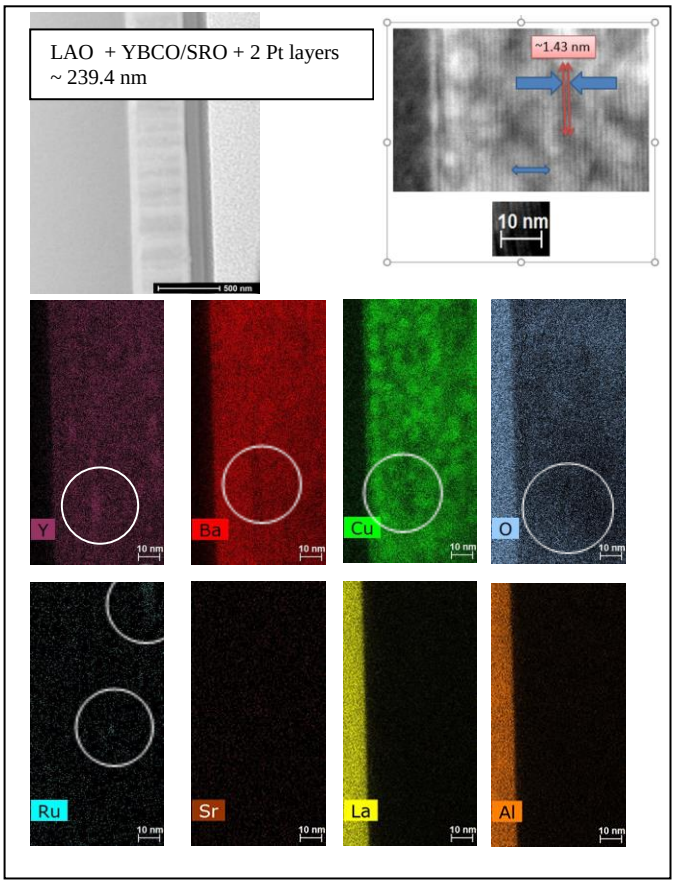

Fig. 1 TEM imaging of 38 bilayers YBCO (~6 nm) / $SrRuO_3$ (~ 0.3 nm) film.

The YBCO/BFO film consisted of 28 bilayers, with a film thickness of 300 nm, with YBCO layers ~11.0 nm per layer, and the BFO comprising 1.4 vol. %. From Fig. 3(b), at 65 K, this film performed better than the YBCO film for fields less than 15000 Oe. Similarly, the BFO doped film performed better at 50 K, at fields less than 32,000 Oe. At 20 K, the BFO/YBCO film performed better than YBCO at fields between 600 and 44,000 Oe, while at 5 K, current density was less than that for YBCO.

The YBCO/YIG film consisted of 38 bilayers, with a film thickness of 254 nm, with YBCO layers ~6.0 nm per layer, and the YIG comprising 3.6 vol. %. From Fig. 3(c), at 65 K, this film performed better than the YBCO film for fields less than 46000 Oe. Similarly, the YIG doped film performed better at 50 K, at fields less than 80,000 Oe. At 20 K, the YIG/YBCO film performed better than YBCO at all fields measured up to 100,000 Oe, while at 5 K, current density was greater than that for YBCO at fields less than 12,000 Oe.

The YBCO/SRO film consisted of 38 bilayers, with a film 1 thickness of 240 nm, with YBCO layers ~6.0 nm per layer, and the SRO comprising 2.4 vol. %. From Fig. 3(d), at 65 K, 50 K, and 20 K, this film performed better than the YBCO film for all fields measured up to 100,000 Oe. However, at 5 K, current density was similar to YBCO at fields less than 400 Oe, but performed below YBCO for greater applied fields.

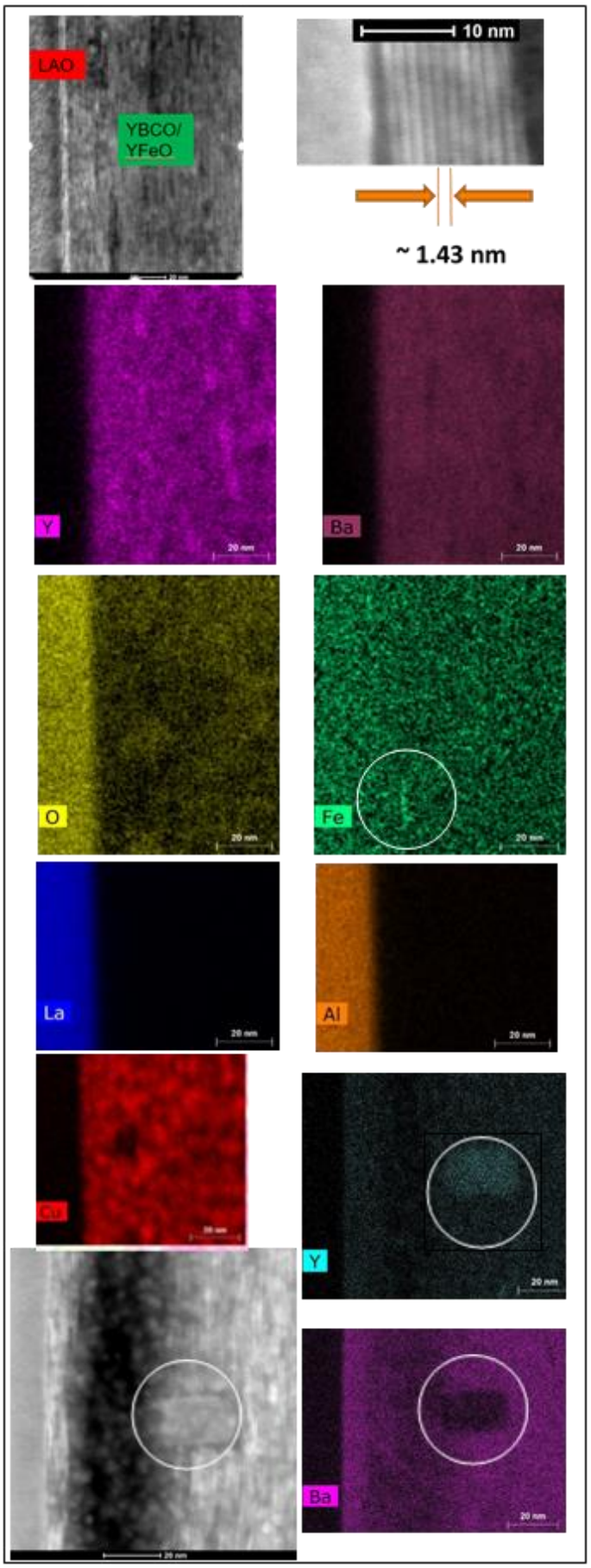

Fig. 2 TEM imaging of 38 bilayers of YBCO (~6 nm) / $Y_3Fe_5O_{12}$ (~0.2 nm) film.

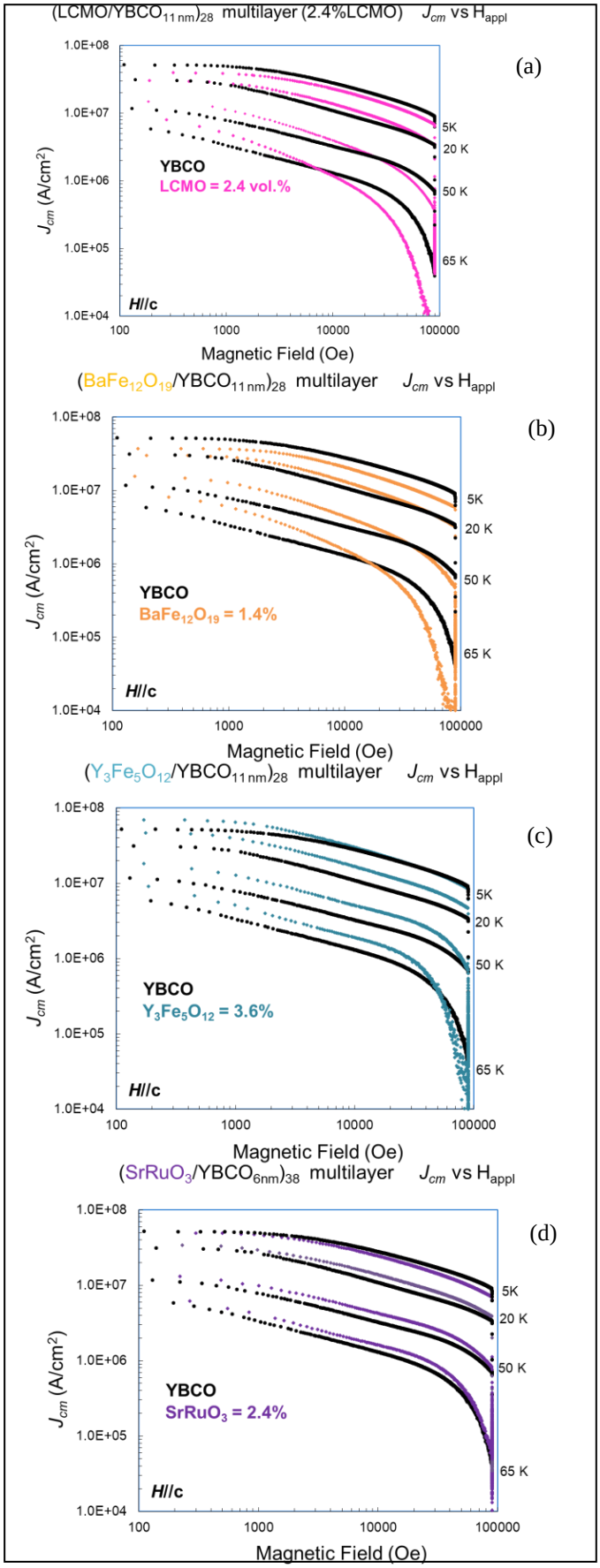

Fig. 3. Current density vs. applied field for multilayer YBCO with a) LCMO, b) BFO, c) YIG, d) SRO layers.

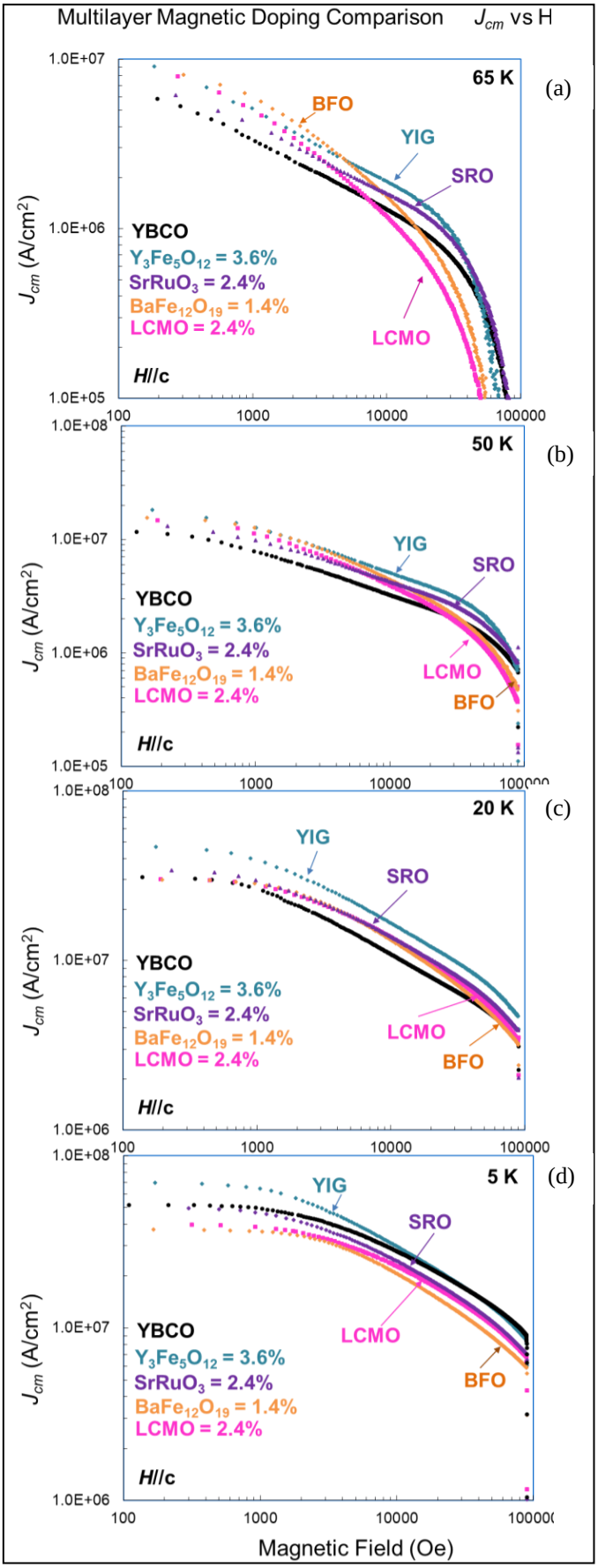

Fig. 4. Comparison of current density vs. applied field for YBCO multi-layer films with LCMO, BFO, YIG, and SRO at a) 65K, b) 50K, c) 20K, d) 5K.

Fig. 4 shows a comparison for all 4 types of magnetic doped YBCO films studied with a separate current density verses field graph for each temperature measured. In Fig. 4(a), at 65K, the BFO doped YBCO film the best for fields less than 5000 Oe. The YIG doped film had the highest current density for fields between 5000–38,000 Oe. At fields greater than 38000 Oe, SRO had the best performance. In Fig. 4(b), at 50 K, the YIG/YBCO multilayer film attained the highest current density up to fields of 73,000 Oe, with SRO performing the best at even greater fields. At 20 K, (Fig. 4(c)), the YIG doped YBCO film reached the highest current density for all applied fields, followed by SRO with the second highest results. For a temperature of 5 K, (Fig. 4(d)), YIG had a higher current density than YBCO for fields less than 17,000 Oe, with similar performance to YBCO at higher fields.

IV. Conclusion

multilayer films consisting of alternating bilayers of magnetic constituents with YBCO, illustrates the presence and benefits of both pinning of the magnetic flux of the vortices and core pinning by nanoparticles and their resulting defects in the film. In addition to the presence of magnetic nanoparticles (LCMO, BFO, YIG, SRO), TEM also revealed the presence of Y_2O_3 nanoparticles, which also contribute to flux pinning. The resultant films grew epitaxially with good crystalline structure, which was confirmed by XRD, T_c, and $T_{c\ FWHM}$ measurements, with the exception of BFO multilayer film. The BFO/YBCO film's T_c degradation may have been due to formation of reaction products. Utilizing magnetic additions increases the pinning capability due to pinning the magnetic flux for fields less than the coercive fields of the additions, while also contributing as nanoparticle core pinning of vortices at fields greater than the coercive fields. The comparison of current density verses field measurement results illustrate the benefit of utilizing the different doped films for different application conditions. Based on these results, BFO/YBCO and YIG/YBCO multilayer films would be suitable for high temperature and low field applications, such as cables. YIG/YBCO and SRO/YBCO would be suitable for mid temperature and mid field applications, such as motors and generators. YIG/YBCO multilayer was the only system studied with good low temperature performance at 5 K, but only surpassed YBCO at fields less than 17,000 Oe. This research leads to a better understanding of the impact of magnetic additions on YBCO film performance, and how it could be utilized for various applications.

REFERENCES

[1] J. P Feighan, A. Kursumovic, J. L MacManus-Driscoll, "Materials design for artificial pinning centres in superconductor PLD coated conductors," *Supercond. Sci. Tech.*, vol. 30 no. 12, Nov. 2017, Art. no. 123001.

[2] K. Matsumoto, P. Mele, "Artificial pinning center technology to enhance vortex pinning in YBCO coated conductors," *Supercond. Sci. Technol*., vol. 23, no. 1, Dec. 2009, Art no. 014001.

[3] L. Opherden, M. Sieger, P. Pahlke, R. Huhne, L. Schultz, A. Meledin, *et al.*, "Large pinning forces and matching effects in $YBa_2Cu_3O_{7-\delta}$ thin films with $Ba_2Y(Nb/Ta)O_6$ nano-precipitates, *Sci. Rep.*, vol. 18, no. 6, Feb. 2016, Art no. 21188.

[4] M. A. P. Sebastian, J. N. Reichart, J. L Burke, L. B. Brunke, T. J. Haugan, C. F. Tsai, *et al.*, "Optimizing flux pinning of YBCO superconductor with dual mixed phase additions," *IEEE Trans. Appl. Supercond*., vol. 23, no. 3, Jun. 2013, Art no. 8002104.

[5] V. F. Solovyov, Q. Li, W. Si, B. Maiorov, T. J. Haugan, J. L. MacManus-Driscoll , *et al., "*Influence of defect-induced biaxial strain on flux pinning in thick $YBa_2Cu_3O_7$ layers," *Phys. Rev. B* vol. 86, no. 9, Sept. 2012, Art no. 094511.

[6] H. Zhou, B. Maiorov, S. A. Baily, P. C. Dowden, J. A. Kennison, L. Stan, *et al.*, "Thickness dependence of critical current density in $YBa_2Cu_3O_{7-\delta}$ films with $BaZrO_3$ and Y_2O_3 addition," *Supercond. Sci & Technol*., vol. 22, no. 8, Jul. 2009, Art no. 085013.

[7] B. Gautam, S. Chen, M. A. Sebastian, T. Haugan, Z. Xing, J. Wu, "Mixed artificial pinning centers by single-doping $BaZrO_3$ and double-doping $BaZrO_3$ + Y_2O_3 $YBa_2Cu_3O_{7-x}$ on flat and vicinal substrates*," IEEE Trans. Appl. Supercond.*, vol. 28, no. 4, Jun. 2018, Art no. 8000104.

[8] M. A. P Sebastian, J. N. Reichart, M. M. Ratcliff, T. J. Bullard, J. L. Burke, C. R. Ebbing, *et al.*, "Study of the flux pinning landscape of YBCO thin films with single and mixed phase additions $BaMO_3$ Z: M= Hf, Sn, Zr and Z= Y_2O_3, Y211," *IEEE Trans. Appl. Supercond.*, vol. 27, no. 4, Jun. 2017, Art. no. 7500805.

[9] T. Haugan, P. Barnes, R. Wheeler, F. Meisenkothen, M. Sumption, "Addition of nanoparticle dispersions to enhance flux pinning of the $YBa_2Cu_3O_{7-x}$ superconductor, *Nature*, vol. 430, no. 7002, Aug. 2004, pp. 867-870.

[10] A. Garcıa-Santiago, F. Sánchez, M. Varela, J. Tejada."Enhanced pinning in a magnetic-superconducting bilayer," *Appl. Phys Lett.*, vol. 77, no. 18, Oct 30, 2000, pp. 2900-2902.

[11] L. N. Bulaevskii, E. M. Chudnovsky, M. P Maley. "Magnetic pinning in superconductor-ferromagnet multilayers, *Appl. Phys Lett.*, vol. 76, no.18, May 1, 2000, pp. 2594-2596.

[12] H. U. Habermeier, J. Albrecht, S. Soltan, "The enhancement of flux-line pinning in all-oxide superconductor/ferromagnet heterostructures, *Supercond. Sci. & Technol.*,vol. 17, no. 5, Feb. 19, 2004, Art. no. S140.

[13] D. Dew-Hughes, M. J. Witcomb, "The effect of dislocation tangles on superconducting properties, *Philos. Mag.*, vol. 26, no. 1, Jul. 1, 1972, pp. 73-96.

[14] C. F. Tsai, Y. Zhu, L. Chen, H. Wang. "Correlation between flux pinning properties and interfacial defects in $YBa_2Cu_3O_{7-\delta}/CeO_2$ Multilayer thin tilms. *IEEE Trans. Appl. Supercond.,* vol. 21, no. 3, 2011, pp. 2758-61.

[15] J. Huang, H. Wang. "Effective magnetic pinning schemes for enhanced superconducting property in high temperature superconductor $YBa_2Cu_3O_{7-x}$: a review," *Supercond. Sci. & Technol*., vol. 30, no. 11 Oct.17, 2017, Art. no. 114004.

[16] M. Gasmi, S. Khene, G. Fillion. "Coexistence of superconductivity and ferromagnetism in nanosized YBCO powders, *J. Phys. Chem. of Solids* vol. 74, no. 10, Oct.1 2013, pp.1414-1418.

[17] Q. X. Jia, P. N. Arendt, S. R. Foltyn, T. G. Holesinger, R. F. DePaula. "Superconducting YBCO films on polycrystalline yttrium-iron-garnet using IBAD-YSZ as a template," *IEEE Trans. on Appl. Supercond*. vol. 11, no. 1, Mar. 2001, pp. 3489-92.

[18] J. Albrecht, S. Soltan, H. U. Habermeier. "Magnetic pinning of flux lines in heterostructures of cuprates and manganites." *Phys. Rev. B*, vol. 72, no 9, Sept. 6, 2005, Art. no. 092502.

[19] R. A. Al-Mohsin, A. L. Al-Otaibi, M. A. Almessiere, H. Al-badairy, Y. Slimani, F. B. Azzouz, "Comparison of the microstructure and flux pinning properties of polycrystalline $YBa_2Cu_3O_{7-d}$ containing $Zn_{0.95}Mn_{0.05}O$ or Al_2O_3 nanoparticles," *J. Low Temp. Phys.*, vol. 192, no. 1–2, Jul. 1, 2018, pp. 100-16.

[20] V. Rouco, R. Córdoba, J. M. De Teresa, L. A. Rodríguez, C. Navau, N. Del-Valle, *et al.*, "Competition between superconductor–ferromagnetic stray magnetic fields in $YBa_2Cu_3O_{7-x}$ films pierced with Co nano-rods," *Sci. Rep.*, vol. 7, no. 1, Jul. 18, 2017, Art. no. 5663.

[21] F. Colauto, M. Motta, W. A. Ortiz, "Controlling magnetic flux penetration in low-Tc superconducting films and hybrids," *Supercond. Sci. & Technol*., vol. 34, no. 1, Nov. 6 2020 Aug 4. Art. no. 013002.

[22] K. S. Pigalskiy, L. I. Trakhtenberg, "Enhancement of intrinsic pinning in the high-temperature superconductor $TmBa_2Cu_3O_y$: Manifestation of the interaction between vortices and a magnetic rare-earth ion," *J. Magn. Magn. Mater*., vol. 497, Mar.1, 2020, Art. no. 165916.

[23] M. A. Sebastian, N. A. Pierce, I. Maartense, G. Kozlowski, T. J. Haugan, "Flux pinning enhancements of $YBa_2Cu_3O_{7-x}$ with nanosize magnetic additions," IOP C. Ser.–Mat. Sci., vol. 756, no. 1, Mar. 1, 2020, Art. no. 012026.

[24] E. J. Kramer, "Scaling laws for flux pinning in hard superconductors," *J Appl. Phys.*, vol. 44, no. 3, Mar. 1973, pp.1360-70.

[25] A. Xu, L. Delgado, M. H. Gharahcheshmeh, N. Khatri, Y. Liu, V. Selvamanickam, "Strong correlation between Jc (T, H‖ c) and Jc (77 K, 3 T‖ c) in Zr-added (Gd, Y) BaCuO coated conductors at temperatures from 77 down to 20 K and fields up to 9 T," *Supercond. Sci. & Technol*., vol. 28, no. 8, Art. no. 082001.

[26] J. W. Kell, T. J. Haugan, M. F. Locke, P. N. Barnes, "Tb and Ce doped Y123 films processed by pulsed laser deposition," *IEEE Trans. Appl. Supercond*., vol. 15, no. 2, Jun. 13, 2005, pp. 3726–3729.

[27] C. P. Bean, "Magnetization of high-field superconductors," *Rev. Mod. Phys*., vol. 36, no. 1, Jan. 1, 1964, pp. 31–39.

[28] C. P Bean, "Magnetization of hard superconductors." *Phys. Rev. Lett*, vol. 8, no. 6, Mar. 15, 1962, p. 250.